This is a repository copy of *Simulation of sheathed cold-formed steel shear walls under lateral load*.

White Rose Research Online URL for this paper:
https://eprints.whiterose.ac.uk/166797/

Version: Published Version

eprints@whiterose.ac.uk
https://eprints.whiterose.ac.uk/

Simulation of sheathed cold-formed steel shear walls under lateral load

S. Kechidi[1], N. Banks[2], O. Iuorio[3]

Abstract

In recent years, new innovative systems have emerged to ensure high structural and environmental performance. Among others, modular cold formed steel (CFS) framed construction has been widely adopted and used in modern, lightweight and cost-efficient engineering practice. The primary objective of this study is to simulate the behaviour of CFS framed shear walls sheathed with oriented strand board (OSB) subjected to monotonic lateral loading (*i.e.*, wind) by means of high-fidelity continuum finite-element (CFE) analyses. A robust three dimensional shell CFE modelling protocol has been developed which aims to provide a benchmark modelling approach able to accurately capture strength, stiffness and failure mechanisms in the above-mentioned structural system. Particular attention was given to the modelling of the sheathing-to-frame screw fasteners where their behaviour were experimentally derived. The proposed modelling protocol has been validated using experimental test results available in the literature, where a good agreement has been achieved. Subsequently, the effect of additional details which are commonly adopted in practice and go beyond the scope of available design guidelines, has been assessed. This includes: (a) the presence of two ledgers (*i.e.*, rim tracks) on the interior face of the shear walls, (b) sheathing boards having different sizes from the overall shear wall sizes and thus the presence of both vertical and horizontal panel seams in the walls and (c) use of cement particle (CP) board at the bottom part of the shear wall, has been carried out. The key parameters which have most affected the lateral behaviour were identified. The developed modelling protocol is intended to provide an accurate experimentally-derived fastener-based computational tool of sheathed CFS shear walls that can extend the current design codes.

1. Introduction

In cold-formed steel (CFS) framed structures, shear walls are the primary lateral load resisting system. They are composed of CFS C-shaped framing members (chord studs, studs and tracks) attached to steel or wooden sheathing using fasteners. The inelastic behaviour that develops in the connection zone between the CFS frame and the sheathing, resulting from bearing between the sheathing and the fasteners and tilting of the fasteners themselves, is the main mechanism of lateral load resistance, providing that inelastic behaviour of the chord studs is prevented through capacity design. This structural component should be designed to provide adequate lateral shear strength and stiffness to the global structure. However, the current version of the Eurocodes does not provide any guidance for sheathed CFS shear wall systems, which hinders the use of this lateral load resisting system in construction practice (Landolfo et al. 2018 [1]). The North American Standard code of practice for seismic design of CFS Steel Structural Systems AISI S400 (2015) [2] represents the main reference for lateral design

of this type of structures. However, in modular housing additional details beyond the scope of AISI S400-15 [2] emerge, including: (a) the presence of a substantial ledger (track) on the interior face of the shear walls, (b) shear wall sizes that do not match panel sizes and thus the presence of both vertical and horizontal panel seams in the walls and (c) use of cement particle (CP) board at the bottom of the shear wall that do not match the thickness of the OSB.

Several research activities on CFS have been carried out in North America by Branston et al. (2006) [3], Cheng Yu (2010) [4], Yu and Chen (2011) [5], Nisreen Balh (2010) [6], Liu et al. (2014) [7] and Jamin DaBreo (2014) [8] through quasi-static experimental tests on CFS-SWP as well as a dynamic test program conducted by Shamim et al., (2013) [9] on two-storey SWPs. Many experimental and numerical research activities were also undertaken in Europe with the aim of gaining a deep understanding of the behaviour of CFS components and broaden their use as a new structural solution. Fülöp and Dubina (2004) [10], Landolfo et al. (2006) [11] and Fiorino et al. (2016) [12] performed

---

[1] Postdoctoral Researcher, School of Civil Engineering, University of Leeds, s.kechidi@leeds.ac.uk
[2] Special Project Director, ilke Homes Ltd., nigel.banks@ilkehomes.co.uk
[3] Associate Professor, School of Civil Engineering, University of Leeds, o.iuorio@leeds.ac.uk

monotonic and cyclic tests on different configurations of sheathed SWPs and diagonal strap-braced walls. The test outcomes underscored the impact of SWP physical and mechanical characteristics on its hysteresis behaviour. The main parameters which have been identified are: the fastener spacing, the sheathing thickness, the height-to-width aspect ratio and the framing thickness of the panel. As far as the numerical aspect is concerned, many FE models have been developed to simulate the hysteresis behaviour of the CFS-SWP. Nisreen Balh (2010) [6] used Stewart model (1987) [13] which accounts for the pinched behaviour and the stiffness deterioration; however, the strength deterioration has not been considered. Jiazhen Leng (2015) [14] modelled CFS-SWP using Pinching4 hysteresis model based on test results carried out on isolated SWP, then, two-storey CFS framed building was modelled for the assessment of its seismic performance employing the calibrated SWP model parameters. The Bouc–Wen–Baber–Noori (BWBN) (1993) [15] model was used by Nithyadharan and Kalyanaraman (2013) [16] to capture the deteriorating behaviour, in terms of the strength and stiffness deterioration with severe pinching, which has been observed in the screw fasteners between the CFS framing members and the sheathing under cyclic loading. Based on the dynamic tests results of two-storey SWP obtained by Shamim and Rogers (2013) [17], the Pinching4 model has been calibrated. Vigh et al. (2014) [18] presented model development and calibration to tests results through a simplified strut model to represent the CFS corrugated steel-sheathed SWP in global structural analysis. The calibration of nonlinear model parameters to experimental data uses genetic algorithms optimization method. The model allows to capture the monotonic as well as the cyclic performance of the SWP. In order to take into account the simulation of the effect of cyclic deteriorations, the Ibarra-Medina-Krawinkler model is applied. Buonopane et al. (2015) [19] developed and validated a FE model for the simulation of CFS-SWPs using OpenSees software; it consists of beam-column elements for the CFS framing and a rigid diaphragm for the sheathing. The sheathing-to-framing connections are modelled using CoupledZeroLength elements having nonlinear uniaxialMaterial (Pinching4) model which captures the sheathing material damage in the area surrounding the fastener. This modelling technique provides detailed information on forces in the framing members and developed strengths at individual fasteners. David Padilla-Llano (2015) [20] proposed a numerical framework for CFS-SWPs that captures the nonlinear cyclic behaviour of critical components including axial members as well as screw fasteners. Firstly, the cyclic experimental and characterisation of axial members was incorporated into a uniaxialMaterial model which follows the same format of the original Pinching4 model introduced by Lowes and Altoontash (2003) [21] with redefined variables to make damage accumulation independent for negative and positive excursions. Then, nonlinear behaviour in critical

components (chord studs) was included in the model developed by Buonopane et al. (2015) [19]. The results from the SWP study highlighted the need to include local buckling behaviour and any other nonlinear behaviour in components when analysing structural systems with thin walled members as it can reveal additional limit states and failure mechanisms that may go unnoticed if not included. All the above-mentioned hysteresis models have parameters which are depending on the conditions and results of the experimental tests and do not refer explicitly to the physical and mechanical characteristics of the CFS-SWP.

Besides, Martínez and Xu (2010) [22] developed a simplified approach for analysing CFS framed buildings using FE method where the SWP is modelled by a 16-node shell element having equivalent material properties. The nonlinear behaviour of SWP is characterised by a stiffness deterioration factor which is a function of the spacing of sheathing-to-framing screw fasteners located at the edge of the SWP. However, with no un-loading and re-loading paths defined, the latter could merely be used for a pushover analysis (monotonic loading) rather than a nonlinear dynamic or cyclic loading analysis. Although a variety of experimental studies has been conducted, along with various modelling approaches, to the authors' knowledge high-fidelity finite element methods able to capture the complex lateral response and failure modes of CFS shear walls for a variety of realistic structural configurations and details have not yet been reported.

This work aims to provide a benchmark shear wall modelling approach for sheathed CFS shear walls under lateral loading. For this reason, a robust three-dimensional high-fidelity shell finite element model is introduced and validated by CFS shear wall tests (Section 3). The focal point of this work includes a fastener-based modelling approach to better capture connection failure and including deformation of the sheathing and all the steel components in the wall. The proposed modelling protocol has been validated using experimental test results available in the literature (Liu et al. 2014 [7]), where a good agreement has been achieved. Subsequently, the effect of additional details which are commonly adopted in practice and go beyond the scope of available design guidelines, has been assessed in Section 4. This includes: (a) the presence of two ledgers (*i.e.*, rim tracks) on the interior face of the shear walls, (b) sheathing boards having different sizes from the overall shear wall sizes and thus the presence of both vertical and horizontal panel seams in the walls and (c) use of CP board at the bottom part of the shear wall, has been carried out. The key parameters which have most affected the lateral behaviour were identified. The developed modelling protocol is intended to provide an accurate experimentally-derived fastener-based computational tool of sheathed CFS shear walls for potential use in design code expansion.

2. Nonlinear finite element modelling approach

The commercial FE software ABAQUS 2017 was used to simulate CFS sheathed shear walls (height x width: 2974 mm x 2400 mm) and support conditions. The model and its parts are illustrated in Figure 1. The dimensions of the assembly are established according to future experimental setup. The following sections outline the modelling details including the material model, simulation of geometric imperfections, contact modelling, replication of end conditions from the tests and solution method.
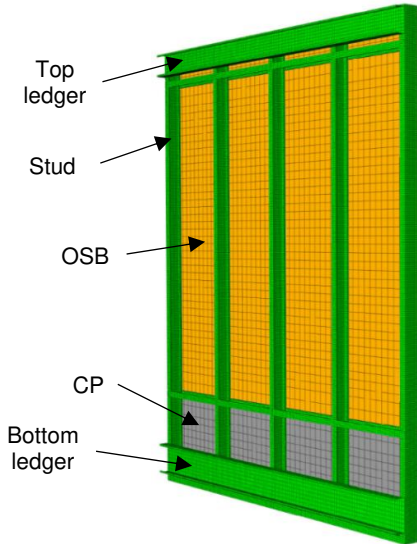

Figure 1: Undeformed ABAQUS models

CFS studs and sheathing are modeled using the nine-node quadratic isoparametric shell element, S9R5, in ABAQUS. The thin shell S9R5 element uses quadratic shape functions

and a reduced integration scheme. Signature curve analyses using the semi-analytical finite strip-based elastic buckling software CUFSM [23] was used to generate the nominal geometries for each specimen, including their corresponding local, distortional, and global elastic buckling mode shapes and wavelength information for use in generating geometric imperfections. All buckling-based imperfection shapes are shown in Figure 2. For the C100-41.3-1.6 single sections, the superposition of a half sine wave of major axis/camber (G2) with a full cosine wave of pure torsion (G3) mode was used to generate a flexural-torsional imperfection, as recommended by Zhao [24]. Kechidi et al. [25] includes a more detailed description of the statistical basis for the magnitudes of each imperfection type (shown here in Table 1, using the modal imperfection decomposition (MID) method) and the specific combinations (including imperfection shape directionality) used for the single and built-up section models which yielded FE analysis results best matching the tested behaviour.
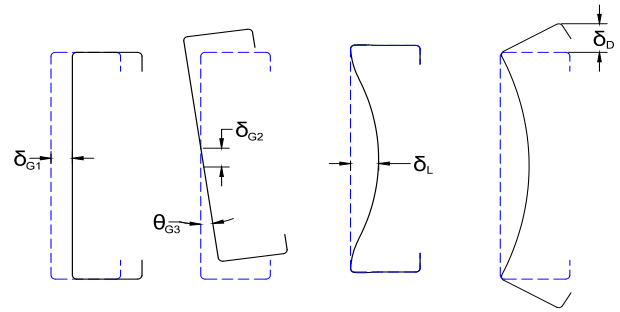

Figure 2: Mode shapes for single sections used for modal imperfections in ABAQUS; from left to right: single global minor axis, flexural-torsional, local and distortional; positive (+) orientations are shown

Table 1: Median buckling mode amplitudes used

Cross Section	Imperfection Database	Local (Type 1)	Distortional (Type 2)	G1[a]	G2	G3[b]
C100-41-1.6	Conventional	1.06t	0.93t	L/692.2	L/761.1	1.017L
	MID	0.58t	0.43t	L/692.2	L/761.1	1.017L

[a]Member's full length L in meters
[b]G3 (torsional) imperfection amplitude calculated in degrees

In-house MATLAB code was used to build shell FE meshes for each specimen, as well as add tracks and fasteners to the model. A fine mesh is used so that all buckling modes can develop with reasonable accuracy. Elements are placed every 5 mm along the longitudinal axis of the studs, tracks and noggins, and 50 mm along the length for the OSB and CP boards. To prevent the element aspect ratio from exceeding 2:1, the mesh requires four elements on the lip and flanges of the channel sections, and 8 elements on the web. All corners are modeled using 4 elements, where the aspect ratio is more difficult to maintain. To characterize material properties, a series of tensile tests were completed

using the steel of the two cross-section types in the study. Testing was completed in accordance with BS EN ISO 6892-1 (2016) [26]. The average yield stress (determined using the 0.2% offset method) and ultimate tensile strengths for the C100-41.3-1.6 section were recorded with a mean of 472.4 MPa and 495.5 MPa, respectively. All yield stress values are considerably above the nominal 450.0 MPa. Young's modulus was not estimated from the linear data in the test results and is assumed to be 203400 MPa as prescribed in EC3 Part 1.3 [27]. A material model using von Mises yield criteria with isotropic hardening was employed.

Measured data was converted to true stress and true plastic strain using Eq. 1-2.

$$\sigma = s(1 + e) \qquad (1)$$
$$\varepsilon_{plastic} = ln(1 + e) - \frac{\sigma}{E} \qquad (2)$$

Where:
σ and s are the true and engineering stresses, respectively, ε and e are the true and engineering strains, respectively, $\varepsilon_{plastic}$ is the true plastic strain with the elastic strain component subtracted, and E is Young's modulus.

Surface-to-surface contact using the finite-sliding tracking method was used to define the interaction relationship between the webs of the channel sections and between the channel section flanges and the OSB/CP when present. Interpenetration of these shell elements was prevented. The general contact algorithm uses a "hard contact" formulation and the penalty method is used to approximate the hard pressure-overclosure behaviour. Friction was also modeled, and the coefficient of friction was taken as 0.19 (for steel-steel and steel-OSB/CP).

The out-of-plane support of the top track in the experiments was included in the model as transverse roller constraints. The wall under shear is expected to have only in - plane displacements. Therefore to avoid any out-of-plane displacement, the top track was constraints with transverse roller constraints, and all nodes on the web of the top track are fixed in the transverse direction.

The anchor bolts connecting the bottom track to the foundation are modeled as pinned connections by fixing all nodes on the web of the bottom track in both horizontal and transverse direction. This allows force in the shear wall to be transferred directly to the foundation in these two directions. Hold-downs are considered to anchor the wall at each end to prevent overturning. Hold-downs are usually realized with high strength steel, and as demonstrated by previous research (Iuorio et al 2014), they are over strength and do not deform when the wall is subjected to in plane loads. Therefore, hold-downs are modelled so that all the nodes in the areas on the web of chord studs which are connected to the hold-down are bound into a rigid body and a single node at the centroid of these areas is assigned to the rigid body (Figure 3). As a result, the movement of this collection of nodes will be governed by the movement of the rigid body reference node. Therefore, the relative positions between the constituent nodes remain constant during the simulation and the whole area does not deform but undergoes a rigid body motion. In order to simulate the threated rod that connects the hold-down to the ground, a vertical bilinear spring is used to connect the rigid body reference node to a node on the ground. This modelling choice is based on the study of Buonopane et al. (2015) [19] in which the necessity

of modelling the tension flexibility of the hold-down is demonstrated. Herein, the tension stiffness of the hold-down is selected to be 9930 kN/m based on Jiazhen Leng (2015) [14]. The compression stiffness is chosen to be 1000 times larger than the tension stiffness based on the assumption that axial force in chord studs is transferred rigidly to the foundation when the hold-down is in compression. The bi-linear spring connecting the reference node to a node on the ground is modeled by means of nonlinear spring element type SPRING2 in Abaqus. This type of element is used to connect two nodes and allows the definition of nonlinear behaviour for a fixed degree of freedom of interest. This nonlinear behaviour can be defined by providing pairs of force relative displacement values. It is important to note that these values need to be given in ascending order of relative displacement. Also, a non-zero force needs to be assigned at zero relative displacement.
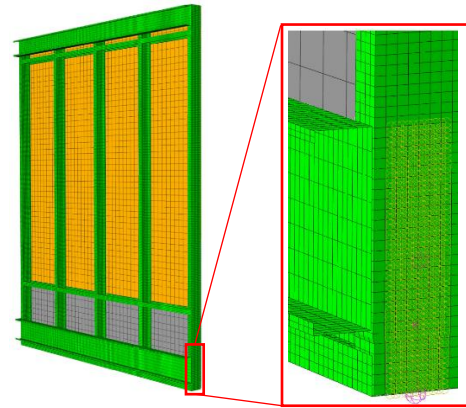

Figure 3: Modelled hold-down

Although the static-Riks solver is typically preferred for static, monotonic loads applied to models with thin shell elements, convergence and/or post-linear behaviour was difficult to achieve in most of the models analyzed in this study. Static-General also did not typically converge post-peak in some analyses, adequate results were obtained using an artificial damping factor of 1×10^{-6}. In search of a solver that could yield capacities and deformations that agree well with test results and that could achieve convergence, the dynamic-implicit solver in ABAQUS, with a quasi-static application type, was adopted for this work. The only additional input for this solver is density for cold-formed steel, which is taken as 7850 kg/m^3 (ASTM A1003). Since a higher order element (S9R5) was employed in the analysis, a consistent mass matrix is developed for each element. No damping factor was required for this solution technique. The dynamic implicit is robust and can improve convergence behaviour for problems involving large nonlinearities (material and/or geometric), contact modelling, and moderate energy dissipation in quasi-static loading conditions. It is also well-suited for determining an essentially static response in monotonic and cyclic loading conditions.

4

A small parametric study on a sample specimen was completed to analyze the effect of solution technique type on peak load, load-displacement behaviour, and convergence ability. Figure 4 shows that all solution techniques could output peak lateral capacity of the simulated shear wall and some post-peak behaviour for this wall, at least until an 15% post-peak level, if convergence was reached.
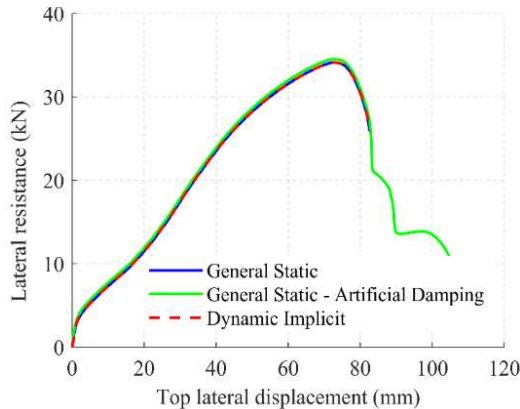

Figure 4: Comparison of shear wall behaviour obtained using three different solvers implemented in ABAQUS

Results of peak capacity as well as resistance vs. displacement behaviour using the dynamic implicit solver are shown in Figure 4 and compare well with results obtained using static general and static-general with artificial damping. A 3% increase in peak capacity is observed when using the static-general with artificial damping method, comparing with the peak loads in the other analyses. The static-Riks based response curve did not proceed more than two increments beyond the peak load due to lack of convergence and analysis termination.

The artificial damping approach removes (artificially) energy from the system as a means of dissipating the nonlinearities that are inherent in the model. It should be noted that this algorithm is quite robust and the author has observed numerous cases where the arc-length (Riks) solver failed to converge, but artificial damping provided a converged solution. Nonetheless, the solution from the artificial damping method is by its nature an approximation. This approximation should be used with great care. Therefore, this type of solver was only adopted for critical cases (*e.g.*, dense screw spacing).

3. Validation of the modelling protocol

Lateral loading is introduced at the top of the wall as displacement control. A displacement of 120 mm is assigned as a boundary condition at a reference point (RP) at the center of gravity of the upper track. The reference point is tied at one edge of the track cross-section using the RIGID BODY command from ABAQUS library. The default nonlinear solution Newton-Raphson method in ABAQUS is used and geometric nonlinearities are included in the analysis. A comparison of the computational results with the experiments is provided herein, emphasizing strength, stiffness and failure modes.

Force-displacement curves for both experimental (blue curve) and computational (red curve) results are shown in Figure 5. The results illustrate that wall strength is accurately captured within less than 3% difference from test results (Liu et al. 2014 [7]). Furthermore, displacement at peak load is captured within 15%. The wall response variance through the FE model is emphasized and further discussed in the following parametric analysis subsection.
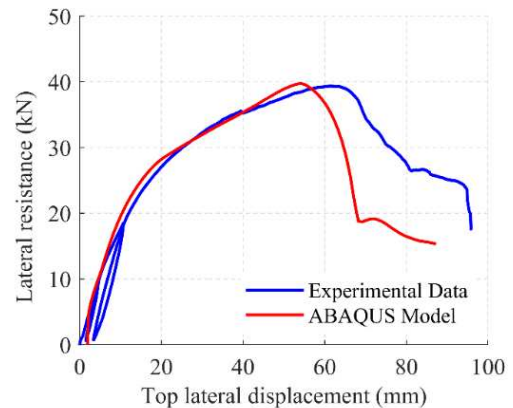

Figure 5: Comparison of tested behaviour of specimen 11c [7] with ABAQUS analysis results

4. Effect of practical aspects on CFS shear wall lateral capacity

Once benchmarked against the physical tests for global load-displacement behaviour, the computational models allow for more detailed study of the response of other similar CFS shear walls. This work, in particular, aimed to study the effect of additional details which are commonly adopted in practice and go beyond the scope of available design guidelines. This includes: (a) number of screws, (b) the presence of two substantial ledgers (*i.e.*, rim tracks) on the interior face of the shear walls, (c) sheathing boards having different sizes from the overall shear wall sizes and thus the presence of both vertical and horizontal panel seams in the walls and (d) use of CP board at the bottom part of the shear wall. The key parameters which have most affected the lateral behaviour were identified.
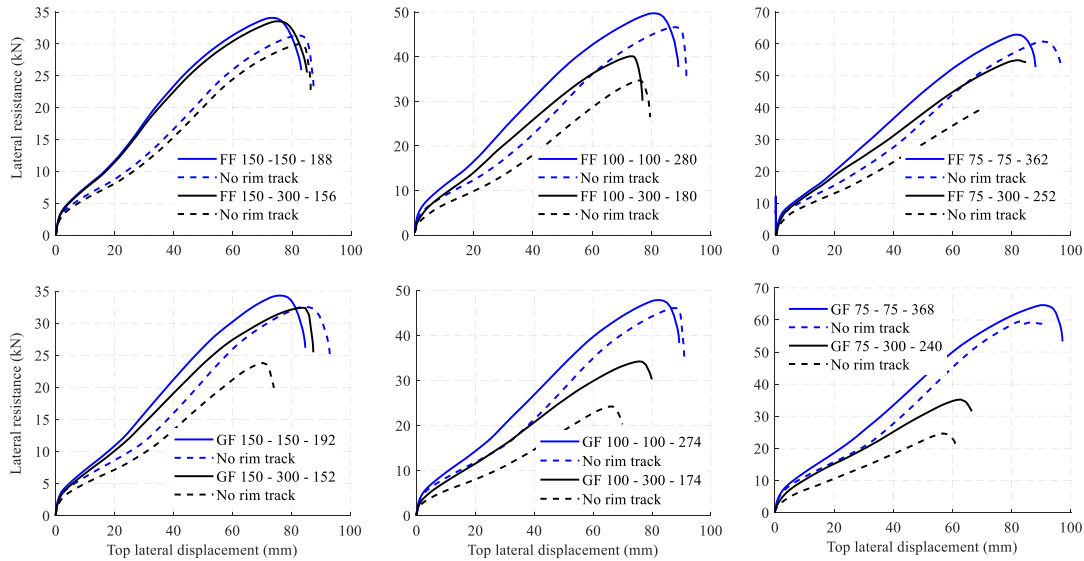
Figure 6: Lateral resistance vs. lateral top displacement curves considering ground and first floors (top and bottom subfigures, respectively), screw spacing (from left to right: 150, 100 and 75 mm) with and without rim track

For both ground and first floor shear walls, a steady increase in shear resistance is associated with screw spacing reduction as illustrated in Figure 6. The initial stiffness increases when the screw spacing decreases, however, the variation is not linear and in some cases, it decreases when putting additional screw fasteners on the perimeter. It should be noted that ductility values are almost unaffected.

The displaced shape shows that the sheathing panels rotating as rigid bodies, while the frame deforms as a parallelogram with some member curvature (due to the two horizontal seems). It can be seen that doubling the screw spacing in the top and bottom stripes (relative the central part of the wall) would results in less drop in the lateral resistance of the wall (see Figure 7).
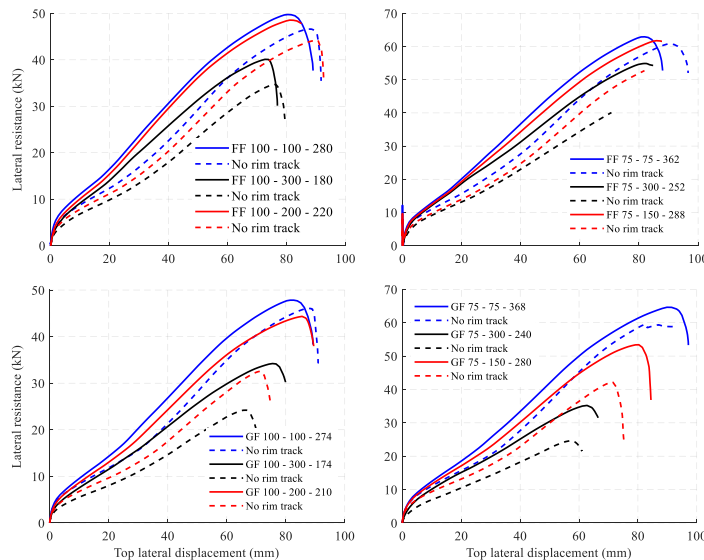

Figure 7: Lateral resistance vs. lateral top displacement curves considering screw spacing (from left to right: 100 and 75 mm) with and without rim track

5. Comparison with design codes

In this section, the results of the above-described numerical simulations are compared to AISI design code (AISI S400-15 [2]) and SCI ED002 [28] prescriptive methods, and percentage differences between computational and code results illustrate that wall strength is captured within 7% (at max) in all of the simulated cases. Strength overestimation is indicated by "+", and strength underestimation by "-". Since OSB-sheathed CFS shear walls are governed by a

6

variable connection response, code prediction for strength capacities based on a few test repetitions may be significantly divergent. The modelling suite detailed in this summary further validates this under/under prediction (Table 2), and motivates recalibration of the existing prescriptive methods and expansion to shear walls not currently included.

Table 2: Wall resistance comparison between ABAQUS model, SCI ED002 and AISIS 400-15 design codes.

Floor level	Screw spacing (mm)	Rim track	Finite element (kN)	SCI ED002 (kN)	Difference (%)	AISI S400 (kN)	Difference (%)
Ground floor	75/75	✓	64.63	63.2	-6	61.67	-4
		-	59.51				
	75/300	✓	35.21				
		-	24.63				
	100/100	✓	47.82	47.4	-3	49.39	-7
		-	46.05				
	100/300	✓	34.22				
		-	24.21				
	150/150	✓	34.30	31.6	+3	32.93	-1
		-	32.53				
	150/300	✓	32.40				
		-	23.79				
First floor	75/75	✓	62.93	63.2	-4	61.67	-1
		-	60.77				
	75/300	✓	54.89				
		-	39.67				
	100/100	✓	49.75	47.4	-2	49.39	-6
		-	46.62				
	100/300	✓	40.10				
		-	34.69				
	150/150	✓	34.08	31.6	-1	32.93	-5
		-	31.35				
	150/300	✓	33.54				
		-	30.00				

6. Conclusions

The conclusions and the impact of this work are multifaceted in both CFS research and design code applications. This study firstly quantifies the connection behaviour between CFS components and OSB sheathing. Two failure mechanisms govern the connection response; screw tilting and pull through. Localized sheathing bearing accompanies both failure modes. Another important finding of this work lies in the efficiency of fastener-based computational models to capture OSB-sheathed CFS shear wall behaviour and complex failure modes. Specifically, the introduced high-fidelity modelling approach is able to capture strength, stiffness and fastener-oriented failures modes of different shear wall configurations. The key point of the proposed computational tool is the connection modelling, which recommends or necessitates experimental-determined connections data use for CFS-to-OSB/CP connection in order to accurately capture the full shear wall behaviour. The proposed finite element model not only aims to fill the gap in the research community, but it is also intended to be used for design code expansion given the fact that the current version of the European code for steel structures design, EC3 [26], does not provide any guidance for CFS shear wall system, which limits the use of this lateral load resisting system in construction practice. Furthermore, AISI S400-15 [2] represents the main reference for the lateral design of this type of structures without covering the details studied in this paper and its design applications are limited to specific component thicknesses and fastener patterns. For this reason, the validated computational tool can play a fundamental role towards that direction. This work is also intended to be used as a benchmark and to be expanded into different sheathing materials, such as steel, fiber cement board and sure-board for both CFS shear wall and CFS diaphragm finite element modelling with a potential use on full building capacity predictions and design.

7. Acknowledgments

References

[1] Landolfo R., Iuorio O., Fiorino L. (2018). Experimental seismic performance evaluation of modular lightweight

steel buildings within the ELISSA project. Earthquake Engineering and Structural Dynamics. 47, 2921 – 2943.

[2] AISI-S400-15 (2015). North American standard for seismic design of cold-formed steel structural systems. AISI-S400, American Iron and Steel Institute, Washington, D.C.

[3] Branston, A. E., Chen, C. Y., Boudreault, F. A., and Rogers, C. A. (2006). Testing of light gauge steel-frame-wood structural panel shear walls. Canadian Journal of Civil Engineering, 33(5), 561 – 572.

[4] Yu, C., Shear Resistance of Cold-Formed Steel Framed Shear Walls with 0.681 mm, 0.762 mm, and 0.838 mm Steel Sheet Sheathing, Engineering Structures, V. 32, (2010), 1522-1529.

[5] Yu, C. and Chen, Y., Detailing Recommendations for 1.83 m Wide Cold-Formed Steel Shear Walls with Steel Sheathing, Journal of Constructional Steel Research, V. 67, n° 7, (2011), 93-101.

[6] Balh, N., Development of seismic design provisions for steel-sheathed shear walls, Master thesis, McGill University, Montreal, Québec, Canada, (2010).

[7] Liu, P., Peterman, K.D. and Schafer, B.W., Impact of construction details on OSB-sheathed cold-formed steel framed shear walls, Journal of Constructional Steel Research, V. 101, (2014), 114-123.

[8] DaBreo, J., Impact of Gravity Load on the Lateral Performance of Cold-Formed Steel Frame/Steel Sheathed Shear Walls, Master of thesis, Department of Civil Engineering and Applied Mechanics, McGill University, Montreal, Québec, Canada, (2012).

[9] Shamim, I., DaBreo, J. and Rogers, C.A., Dynamic testing of single- and double-story steel sheathed cold formed steel framed shear walls, Journal of Structural Engineering, V. 139, n° 5, (May 2013), 807-817.

[10] Fülöp, L. and Dubina, D., Performance of wall-stud cold formed shear panels under monotonic and cyclic loading Part II: numerical modelling and performance analysis, Thin-Walled Structures, V. 42, n° 2, (2004), 339-349.

[11] Landolfo, R., Fiorino, L. and Corte, D.G., Seismic behavior of sheathed cold-formed structures: Physical tests, Journal of Structural Engineering, V. 132, n° 4, (2006), 570-581.

[12] Iuorio, O., Fiorino, L. and Landolfo, R., Testing CFS structures: The new school BFS in Naples, Thin-Walled Structures, V. 84, (2014), 275-288.

[13] Fiorino, L., Iuorio, O., Macillo, V., Terracciano, M.T., Pali, T. and Landolfo, R., Seismic Design Method for CFS Diagonal Strap-Braced Stud Walls: Experimental Validation", Journal of Structural Engineering, V. 142, n° 3, (2016).

[14] Leng, J., Simulation of cold-formed steel structures, PhD thesis, John Hopkins University, Baltimore, United States, (2015), 827 p.

[15] Foliente, G.C., Stochastic dynamic response of wood structural systems, PhD thesis, Virginia polytechnic institute and state university, Blacksburg, Virginia, United States, (1993).

[16] Nithyadharan, M. and Kalyanaraman, V., Modelling hysteretic behaviour of cold-formed steel wall panels, Thin-Walled Structures", V. 46, (2013), 643-652.

[17] Shamim. I. and Rogers, C.A., Steel sheathed/CFS framed shear walls under dynamic loading: Numerical modelling and calibration, Thin-Walled Structures, (2013), V. 71, 57-71.

[18] Vigh, L.G., Liel, A.B., Deierlein, G.G., Miranda, E. and Tipping, S., Component model calibration for cyclic behavior of a corrugated shear wall, Thin-Walled Structures, V. 75, (2014), 53-62.

[19] Buonopane, S.G., Bian, G., Tun, T.H. and Schafer, B.W., Computationally efficient fastener-based models of cold-formed steel shear walls with wood sheathing, Journal of Constructional Steel research, V. 110, (2015), 137-148.

[20] Padilla-Llano, D.A., A framework for cyclic simulation of thin-walled cold-formed steel members in structural systems, PhD thesis, Virginia Polytechnic Institute and State University, Blacksburg, United States, (2015), 226 p.

[21] Lowes, L.N. and Altoontash, A., Modelling the Response of Reinforced Concrete Beam-Column Joints, Journal of Structural Engineering, V. 129, (2003), 1686-1697.

[22] Martinez, J.M. and Xu L., Simplified Nonlinear Finite Element Analysis of Buildings with CFS Shear Wall Panels, Journal of Constructional Steel Research, V. 67, n° 12, (December 2010), 565-575.

[23] Schafer, B.W. and Ádàny, S., Buckling analysis of cold formed steel members using CUFSM: conventional and constrained finite strip methods, Proceedings of the 18th International Specialty Conference on Cold-Formed Steel Structures, Orlando, FL, (2006).

[24] Zhao, X. (2016). Measurement and Application of Geometric Imperfections in Cold-Formed Steel Members, PhD thesis, Johns Hopkins University, Baltimore, MD., United States.

[25] Kechidi, S., Fratamico, D.C., Schafer, B.W., Castro, J.M. and Bourahla, N., Simulation of screw connected built-up cold-formed steel back-to-back lipped channels under axial compression, Engineering Structures. 206 (2020) 110109.

[27] BS EN ISO 6892-1 (2016) Metallic materials. Tensile testing. Method of test at room temperature. London: BSI.

[26] EN 1993-1-3, Eurocode 3. Design of steel structures, Part 1.3: general rules for cold formed thin gauge members and sheeting, European Committee for Standardization, Brussels; CEN (2007).

[28] SCI ED002 (2003) Lightweight steel/timber composite solutions: information and guidance for new product development. Steel Construction Institute, UK.

8